1   **Process Understanding in Freeze-Drying Cycle Development: Applications for Through Vial**

2   **Impedance Spectroscopy (TVIS) in Mini-Pilot Studies**

3   *Geoff Smith[1], Muhammad Sohail Arshad[1,2], Eugene Polygalov[1], Irina Ermolina[1], Timothy R McCoy[3],
4   Paul Matejtschuk[4]

5

6   1. Pharmaceutical Technologies Group, Leicester School of Pharmacy, De Montfort University,
7   Leicester, LE1 9BH, UK

8   2. Department of Pharmacy, Bahauddin Zakariya University, Multan, Pakistan.

9   3. Genzyme, (a Sanofi Company), IDA Business park, Old Kilmeaden Road, Waterford, Ireland

10   4. National Institute for Biological Standards & Control (NIBSC), South Mimms, Potters Bar, Herts,
11   EN6 3QG. UK.

12

13   *corresponding author

14

15   Contact details of Corresponding author

16   **Geoff Smith**
17   Professor of Pharmaceutical Process Analytical Technologies
18   **Postal Address:** Pharmaceutical Technologies Group, Leicester School of Pharmacy, De
19   Montfort University, Leicester, LE1 9BH, UK
20   **Contact Number:** +44 116 250 6298
21   **Fax No.:** +44 116 257 7270
22   **Email address:** gsmith02@dmu.ac.uk

23

24

Abstract

The freeze-drying cycle comprises three stages: (1) Freezing, to form ice and to crystallise out any solutes with a propensity to crystallise, (2) Primary drying to remove the ice phase by sublimation, and (3) Secondary drying to remove the remaining unfrozen water which is bound to the remaining matrix of crystalline and amorphous solids. Given the impact of scale on the process outcomes, any freeze drying cycle developed based on mini-pilot studies, will inevitably require measurement technologies for characterising each stage of the cycle at each scale of the process. However, there are inherent challenges in the development of reliable mini-piloting studies, with the first being the fact that no single PAT technology for freeze-drying may be implemented across all levels of scale, and the second being the inherent changes in process characteristics (process parameters that result from scale up). Here we present a new approach for process understanding in freeze-drying cycle development, which uses a through vial impedance measurement to characterise a broad range of features of the process, including, ice onset times, the completion of ice solidification, the glass transition, and the structural relaxation of the amorphous solid, a surrogate for primary drying rate and the primary drying end point. The on-going development of this technology may see the application with micro-titre plate technologies for formulation screening (micro-scale down) and for scale up into production by using a non-contact probes for monitoring problematic regions within the dryer.

Key Words: Freeze drying, in-line process control, PAT, QbD, critical process parameters

46   **Introduction**

47   The scale up of a lyophilisation cycle is challenging due to multiple differences between

48   small scale and large scale dryers. There is some guidance to facilitate the development of an

49   efficient lyophilisation cycle in the laboratory (1), however, even an optimized cycle from a

50   laboratory freeze-dryer may not transfer smoothly to the manufacturing scale. In addition to the

51   scalability differences, there are several other differences between laboratory and manufacturing

52   scale lyophilisers, which may pose a serious challenge for scale-up. These challenges include: (i) Ice-

53   nucleation differences during freezing, (ii) Heat and mass transfer differences, and (iii) Differences in

54   primary drying time. These differences between laboratory and manufacturing scale lyophilisers can

55   pose a serious challenge and therefore a systematic approach is needed to ensure a smooth scale-

56   up.

57   There are a number of stages in a typical lyophilisation process: Freezing (sometimes

58   including annealing) which transforms the liquid solution into a stable frozen matrix, primary drying

59   to remove the ice, and secondary drying to remove residual water from the unfrozen super-cooled

60   liquid domains of the material [1]. Whilst on the surface these stages appear to be somewhat

61   discrete, they in fact constitute a sequential series of inter-dependent events. The process kinetics

62   (ice formation, sublimation, and moisture desorption) are driven by a number of factors, including

63   heat transfer through the vial base and walls (impacted by any thermal heterogeneities in the shelf

64   temperature and radiant heating on the edge vials), the structure of frozen matrix which evolves

65   from the stochastic ice formation process and the initial water content of the interstitial spaces [2].

66   Any attempt to investigate the freeze drying process is complicated by the fact that the process is

67   undertaken in a closed-system, under extremes of temperature and pressure settings, within a batch

68   of vials in close proximity to each other and many (> 10,000) in number, meaning that direct access

69   by any PAT sensors is limited.

70 It is also widely recognised that any attempt to predict product scale process parameters from the

71 laboratory scale is complicated by the fact that the scale of the operation has a significant impact on

72 the process outcomes. There will be variations in the process parameters, and hence the dependent

73 critical quality attributes, that are considered to be a function of the process scale and care should

74 be exercised to avoid developing a cycle at the mini-pilot scale that cannot be translated to the large

75 scale production [3].

76   It is nevertheless the intention within a scale down/scale up approach to use intermediate or

77 benchtop-scale studies to gain product and process knowledge that helps predict the behaviour

78 (scale-up), assess risks (risk analysis), and diagnose production issues (troubleshooting) at

79 production scales. There will inevitably be limitations to what can be achieved but so long as various

80 factors are considered in the design of a meaningful mini-pilot study then one may be able to

81 maximise the relevance of mini-pilot data to the larger scale production process [4]. The factors to

82 be considered have been discussed elsewhere [5] but include:

83 **1. Formulation composition** - For instance, incomplete crystallization of excipients such as mannitol

84 or glycine [6] with consequential heterogeneity in moisture, crystallinity and appearance.

85 **2. The freezing step** as it defines the ice crystal size, which then defines the pore size for sublimation

86 to occur[7]. Variations in freezing rates associated with differences in temperature at locations

87 around the dryer, coupled to the stochastic nature of super-cooling and nucleation, inevitably

88 introduce heterogeneity [8]. Controlled nucleation is showing promise in delivering shorter primary

89 drying times and greater product homogeneity [9]. Mini-piloting studies might therefore aim to

90 simulate the controlled nucleation that is sometimes practised at the larger scale in an attempt to

91 understand the fast kinetics of the process. However, that may require the development and

92 implementation of new forms of measurement system to track those bulk nucleation and growth

93 phases which result in less efficient secondary drying due to lower surface area.

94 **3. Cycle design & –System Capabilities** – Where a cycle is designed at laboratory or pilot level, the

95 process conditions applied cannot always be achieved in the same way within an industrial scale

96 unit, owing to a number of factors: (i) The rate at which vacuum can be applied may be different

97 between a laboratory system and a production model, especially where process routines require oil

98 free (Rootes) pumps; (ii) The nature of the valve between the chamber and the condenser can also

99 differ between small units (where indeed for some lab models the condenser is inside the chamber)

100 and production units; (iii) The design of the valve and its speed of response, as well as length and

101 diameter of vapour duct, must be taken into account as potential sources of variation on scale up

102 and indeed may make pressure rise testing impractical; (iv) Cooling/heating rates of a mini-pilot

103 dryer and a large process scale machine may differ significantly with the latter only being able to

104 achieve low rates of temperature change owing to the thermal inertia of a large dryer; (v) There may

105 be a significant difference between the temperature achieved on one shelf and another of a large

106 stack of shelves or the time taken to achieve a given temperature across a large stack may differ

107 from the one observed for a small single shelf mini-pilot unit; (vi) The smoothness or 'roughness 'of

108 the finish on the shelves and the flatness of the shelves are factors which must be considered as the

109 creation of a space between the shelf and the base of the vial will influence heat transfer from the

110 shelf to the product. These factors would be difficult if not impossible to model at small scale.

111 Instead, the freeze drying cycle for a production scale dryer may require adjustment in the shelf

112 temperature and chamber pressure in order to achieve the target product temperature.

113 **4. Impact of scale on sublimation rate** The design of a freeze drying cycle for process scale, if based

114 strictly on a mini-pilot data may be too ambitious for the reasons above. Calculation of the heat

115 transfer properties of the freeze drying system, thermal co-efficient of the vial, resistance to vapour

116 flow posed by dry cake, and the gradient in pressure between sublimation front and condenser

117 allow greater predictability to the scale up (1,2,7,8). In primary drying, it is essential that the product

118 temperature is maintained as high as possible in order to maximise sublimative cooling and reduce

119 the primary drying time, while maintaining the product temperature below certain critical

120 temperatures (the eutectic temperature (crystalline) or glass transition (partially or fully amorphous)

121 in order to avoid melt-back or collapse. Engineering factors to consider in process optimization and

122 scale up include: (i) Minimum achievable pressure as a function of sublimation conditions; (ii)

123 Maximum sublimation rates before losing control of pressure or choke flow; (iii) Condenser

124 temperature; as the driving force for sublimation is the pressure gradient due to the pressure at

125 sublimation surface of the product and the pressure at the surface of the ice on the condenser coil;

126 (iv) The vial heat transfer co-efficient- conduction (heat vial contact between the vial base and the

127 shelf); (v) Convection (heat transfer through gas phase); (iii) Radiation (heat transfer from walls,

128 underside of the upper shelves, etc.); (vi) The amount of radiant heat entering through the

129 transparent Perspex door of the freeze dryer, the scale of the shelves and the heat radiated from the

130 walls are all likely to be very different between a mini-pilot dryer and a process dryer while

131 formulation, vial and stopper format remain constant. The impact of shelf, the effect of nearest

132 neighbour interactions and the impact of radiant heat from the shelves above (and hence the inter-

133 shelf distance) are all factors to bear in mind on scale up [10]. The mapping of sublimation

134 heterogeneity across a shelf has been well demonstrated, with the centre of a tray of vials and

135 indeed the centre tray of a series of vials on a shelf, drying more slowly than those at the extremities

136 where external heating effects are greater. Radiation is the dominant mode of heat transfer during

137 lyophilisation [11] and the edge vial experience most radiation, hence the increased product

138 temperature and therefore rate of sublimation for the edge vs centre vials.

139 **Process monitoring and Process Analytical Technology (PAT)** It is clear that the prudent use of

140 process analytical technology (PAT) is a key factor in being able to achieve an effective scalable

141 freeze drying cycle. There are many different technologies for monitoring and even controlling the

142 freeze-drying process, and these have been reviewed elsewhere in a number of comprehensive texts

143 [12-17, 3]. However, these technologies have not been reviewed within the concept of mini-piloting

144 which includes the use of emerging physical characterization techniques that could significantly

145 improve the measurement of process parameters and product quality attributes during drug

146 development and manufacturing that would potentially replace or supplement traditional

147 approaches in the near future.

148 The inevitable question therefore is "which technologies could be used for mini-piloting

149 studies?" Before addressing that question it is worth stating that mini-piloting studies in freeze-

150 drying may take on a number of forms, in terms of the scale length being investigated. Here we

151 define a number of sample and batch scales which could be considered for the concept of a mini-

152 piloting study: 1. Mini-vials and microtitre plates (< 1 ml)[1] in which the size of the sample and

153 container is reduced from that expected of the final product; 2. Single vials (2- 50 ml)[2] to be used for

154 a fill volume to be used for the final product; or 3. Clusters of these vials (modelling the impact of

155 radiant heat from the walls of the dryer) where the total volume for each study is defined by the

156 number of vials in the cluster multiplied by the fill volume.

157 Mini-vials and microtitre plates have been used to effect for high throughput formulation

158 screening [18-22]. However, due to the fact that the change in sample size in relation to container

159 geometry (wall and base thickness and materials of construction) has a significant impact on the

160 freezing and drying processes, which is currently difficult to model, then such systems may not be

161 considered presently for a mini-pilot application. Moreover, the commercial sample scale is

162 determined by the product requirements and is not therefore considered as a variable in the

163 development process: Once the formulation has been selected (with or without the use of a high

164 throughout methodology), the process is developed based on a predefined container size and fill

165 volume (and hence fill height). Mini-pilot studies can therefore be considered from a starting point

166 of a single vial.

---

[1] these are not used in production of any commercial product
[2] these are the vials that are currently available for most commercial products

167   Here we make a definition of cluster size in terms of micro cluster and meso cluster in order

168   in order to recognise the fact that edge effects extend over the outer 3-4 rows of vials in a large

169   cluster, which means that all vials in a micro-cluster will dry as edge vials, whereas a meso-cluster

170   will have some edge vials and some core vials. It is invariably the case that, for the early stage

171   process development, where there is a requirement to minimise the solution volume (and hence

172   drug consumed) the impact of edge effects is removed by placing the product containing vials at the

173   centre of an array of empty vials.

174   Having clarified the definitions and the impact of scale length in terms of numbers of vials, one

175   then can delineate which PAT might be useable for each scale. Table 1 list a number of commercial

176   PATs and research tools that have been defined as being suitable for each of these scale lengths,

177   whereas others have been excluded. As stated above, it could be argued that microplates and mini

178   vials are best suited for initial formulation screening [18] and their use in predicting scale up is quite

179   limited. These systems are therefore excluded from the scope of a mini-pilot study. Given that mini-

180   piloting must start form a single vial, then one might expect that the model single vial systems that

181   have been described and the 7 vial model lyophilizer might be useful in this regard [23]. However,

182   the use of such systems for a mini-pilot study should be used with caution owing to the fact that a

183   single vial (or a micro-cluster of 7 vials) will behave very differently to a vial in the centre of a meso-

184   cluster or a macro-cluster. The impact of radiant heating on the drying characteristics (shape of the

185   drying front and product temperature) are significantly different for a lone vial to a vial within a large

186   cluster.

Table 1 Comparison of analytical technologies for assessment of critical quality attributes and process parameters. The table includes both commercially available systems and those which are currently available only in specific research laboratories.

Sample presentation	Stage	Potential PAT	Excluded PATs
Micro-titre plate	Formulation screening	Uv-vis, Raman, fluorescence, TC	Pressure rise, TDLAS
Single vial	Mini-Pilot Scale to Pilot Scale	OCT, TVIS, NIR, Raman, RTD, TC, Microbalance	Pressure rise, TDLAS
Micro-cluster (7, 19,37 vials)	Mini-Pilot Scale to Pilot Scale	• TC, RTD, TVIS, smart sensor, • NIR & Microbalance ("Edge" vial only)	Pressure rise, TDLAS
Meso-cluster (61,91,127,169+ vials)	Pilot Scale	• TC, RTD, TVIS • TDLAS & pressure rise (demand a minimum number of vials) • NIR & Microbalance ("Edge" vial only)	
Macro-cluster (10,000+ vials)	Production	TC, Pressure rise, TDLAS	Microbalance

NIR: Near infrared, TC: thermocouple, ideally wireless; TVIS: Through vial impedance spectroscopy, OCT: Optical computer tomography. RTD: resistance temperature detector.

It is clear that each PAT technology is somewhat limited in its application across all scales within the development cycle and it remains the case that there is no single PAT technology that can be applied to assess all quality attributes of the product and process parameters of the cycle, at all levels of scale. There are a number of reasons for that, with each pertaining to the PAT in question and the target process parameter for that particular technology. Two process parameters (critical temperatures and drying rates) and one material attribute (glass formation) are used to illustrate this point.

Critical temperatures Single vial systems have been developed for the purpose of evaluating other more novel process analytics, e.g. OCT (optical coherence tomography) measurements of collapse [19]. These are beneficial as they demonstrate a minimum requirement that the analysis of some process parameter or material attribute should be conducted, at least within a container and sample volume that is consistent with that being freeze-dried at the larger scale. This implies that techniques such as conventional freeze-drying microscopy (FDM) may not accurately define the critical parameters (temperatures required to control the process), however they are used extremely frequently and widely in the formulation characterisation process [24].

209   In attempting to drive process efficiencies one tries to maintain the product temperature as

210   high as possible in order to supply the latent heat of sublimation. However this is complicated by the

211   following issues: The product temperature is always lower than the shelf temperature owing to the

212   heat absorbed from the sublimation of ice and the fact that is difficult to measure the temperature

213   at the sublimation interface. TCs placed in the base of the vial can be used to assess the end point of

214   primary drying (for example) but their position at that point precludes the assessment of the

215   temperature at the sublimation interface, which inevitable moves down the vial contents as the

216   drying process progresses. A technique that can measure the product temperature at the ice

217   sublimation front will inevitably provide greater assurance that the temperature at the sublimation

218   interface does not fall below the critical temperature at which the dry layer (in immediate contact

219   with the sublimation interface) does in fact collapse. The implementation of such a PAT tool within

220   the process control loop will inevitably reduce the risk of product failure through over-aggressive

221   drying profiles. In addition, single vial TCs only provide information on thermal events (and the end

222   point of drying) but not the drying rate.

223   **Primary Drying Rates**

224   Pressure rise and TDLAS techniques are used for the measurement of mass flux and drying rates

225   within dryers that are either partially or fully loaded. However, the determination of drying rates as

226   a function of the location of the vial within a cluster is not accessible with these technologies. A

227   commercially available alternative, i.e. the microbalance, can work at the scale of a single vial but

228   only works on an isolated vial or one which is on the edge of a cluster (which inevitably experiences

229   greater radiant wall effects and does not simply rely on heat transfer through the base). Drying rates

230   and dry layer product resistance calculated by this technique therefore should be used with caution

231   when applied to the behaviour of the same materials when freeze-dried within clusters, owing to the

232   significant impact from radiant heating of the side of the glass vial. It is also the case that single vial

233   spectroscopies cannot be used on clusters of vials; any information on product quality (e.g. protein

234 folding by Raman) and water content during drying cannot be easily translated to populations of

235 vials (because the probes are large and will inevitably cause significant disruption to the thermal

236 heat treatment experiences by vials embedded with a manufacturing scale cluster). It is also

237 apparent that existing PATs are limited in their ability to "look inside" the vial with most optical

238 spectroscopy being limited to a surface measurement of 1-2 mm at best. That said, the application

239 of optical spectroscopy for single vial measurements is the subject of renewed interest, given the

240 potential application in the freeze-drying of vials in a continuous process, where such technologies

241 are expected to excel [25-27].

242

243 **The amorphous state (Mesoscopic properties and Glass Formation)**

244 PATs which enable the measurement of mesoscopic properties (i.e. the material properties at the

245 scale length of molecular clusters) such as the glass transition and the fragility/strength of the glass

246 are desired as these properties have significant impact on the product and process efficiency. The

247 formation of the amorphous phase depends to a large degree on the amount of ice that in turn

248 defines the water content of the unfrozen fraction. In addition, the rate at which the amorphous

249 state forms and the temperatures at which the amorphous phase forms will inevitably influence the

250 enthalpy entrapped within the interstitial phases. The power of molecular vibrational spectroscopies

251 has been well-demonstrated [27] These parameters impact the secondary drying phase [28] and

252 even the stability of the glass matrix that forms [29].

253 **Application of PAT across the scales**

254 One key requirement might be that the prospective analytical technology in question has itself

255 a potential for scale up [30]. The principle drawback of mass-flow based PAT techniques is that

256 these display only one temperature value for the entire batch and do not take into account the

257 inter-vial heterogeneities in different locations of the shelf, which are evidenced through individual

258 temperature sensing devices. Generally, the product temperature values obtained from the MTM

259   technique (used for small scale) are believed to be related with the colder region of the shelf that is

260   non-edge or centre of the array and that temperature as low as −45°C during primary drying may be

261   determined with this technique [31]. End point of primary drying is characterized by a sharp drop in

262   vapour pressure of ice. MTM lead product temperature measurement has been fairly representative

263   with first 2/3rd of the primary drying time however after this time heterogeneities in the rates of ice

264   sublimation amongst vials located at different position in the shelf are predominant [32]. Therefore

265   the PAT measured product temperature after this point of time may be non-representative of the

266   actual product temperature [32, 12]. Furthermore the heat transfer rates were misleading when

267   lyophilisation cycles were performed at very low temperatures and low pressure [33] using low solid

268   contents [31] while a minimum sublimation area of 150 cm^2 is required for an accurate MTM

269   product temperature measurement. Lyophilisation of the formulations with high amorphous solid

270   contents were measured inaccurately with MTM, especially in the early phase of primary drying

271   resulting in a high drying temperatures due to re-adsorption of vapours in the dried layer due to

272   pressure rise [12, 34]. Lastly, the closure of MTM valve hinders the sublimation process owing to

273   slowed self-cooling which may sequence to collapse if the freeze drying cycle is operated at

274   temperatures close enough to collapse temperature [12] or if extended isolator valve closure

275   periods are used.

276   TDLAS, another PAT measures the rate of sublimation from the whole batch by recording the

277   light absorption during the passage of vapour through the duct connecting drying chamber and the

278   condenser [35, 36] provided the freeze drier requires has a conducting duct of an appropriate

279   length. This can be used in-process to feedback and control of the freeze drying cycle as in the

280   LyoStar (Virtis) range of dryers.

281   Both MTM and TDLAS have been used to develop a series of models for the freeze drying

282   process and also to build those algorithms into the first smart freeze drying processes that allow

283   control on-line to be achieved either by intervention or automatically [37]. However, he application

284   of these tools in mini-piloting of freeze drying process is somewhat limited given the requirement for

285   a minimum batch size.

286   As stated above, mini-pilot data may not translate appropriately through scale up unless the

287   PAT technology used to assess the process is also transferrable between scales, and thereby provide

288   an opportunity to unify the PAT signatures at each scale length. For example, in the case of protein

289   formulations (which are sensitive to freeze-concentration stresses) then mini-pilot data from a single

290   vial or micro-cluster of vials may not translate to larger clusters within bigger dryers because the way

291   the sample freezes could impact factors such as aggregation of the active.

292   Techniques which might bridge the gap between the small-scale (e.g. single vial freeze-dryer

293   to the production scale) are limited. One of the few examples are wireless temperature sensors [38]

294   which are an improvement over classical thermocouple or resistance thermometers owing to the

295   lack of wiring, and compatibility with automated loading systems but they are still very much tools

296   used in development, invasive in nature and perturb the ice formation as well as sublimation kinetics

297   . There is an unmet need for a non-invasive technique that can measure both critical events, such as

298   ice formation, glass transition and solidification and collapse, while being able to measure drying

299   rates and end points, and to able to do that across a range of scales from the single vial to multiple

300   vials within clusters, so that the impact of both vial base and radiant wall heating can understood in

301   terms of its impact on process parameters and critical quality attributes. In essence, it is essential

302   that both core and edge vials are assessed for conformity with specification so that the mini-pilot

303   data can be assessed in terms of its direct relevance to production scale and that risks to product

304   quality are understood and mitigated. A more recent PAT technology based on through-vial

305   impedance spectroscopy (TVIS) has been introduced to partly fulfil this need. This technology is non-

306   contacting to the product (unlike an invasive impedance probe in a vial (such as CHRIST's LyoControl

307   technology [39]) and provides some opportunity to characterize material properties across the

308   scales. Albeit in its current form it is a single vial measurement, the opportunity exists to use

309   multiple sensors to track different regions of the dryer and at different scale lengths; and in future

310   the potential development of a non-contact format may allow for such measurements in both scale

311   down application (within mini-vials or micro-wells) and for scale up for multi-vial clusters. The latter

312   is currently the subject of a UK government funded, Innovate UK project called "Biostart".

313   Theoretical feasibility has been established and a demonstrator unit is currently under development.

314   **Through-Vial Impedance Spectroscopy (TVIS)**

315   Impedance monitoring has a long history as a lyophilisation analysis tool [40, 41]. TVIS

316   measures the electrical impedance of the product, contained within a standard freeze-drying vial

317   that has been modified with electrodes placed on the outside of the glass wall [42]. The impedance

318   measurement vial is connected to a low input-impedance, current to voltage convertor (IVC), via a

319   junction box within the freeze-dryer chamber (mounted close to the shelf on which the vials are

320   located). The signals from the stimulating voltage and that from the resultant current (from the I-to-

321   V convertor) [43] are compared in order to determine the impedance of the measurement vial (and

322   its contents) (Figure 1). The calibration of through vial impedance measurement system is

323   performed by taking in account the impedance contribution at open loop as well as close loop

324   conditions using a reference standard of known capacitance. Details are described in the literature

325   [42].
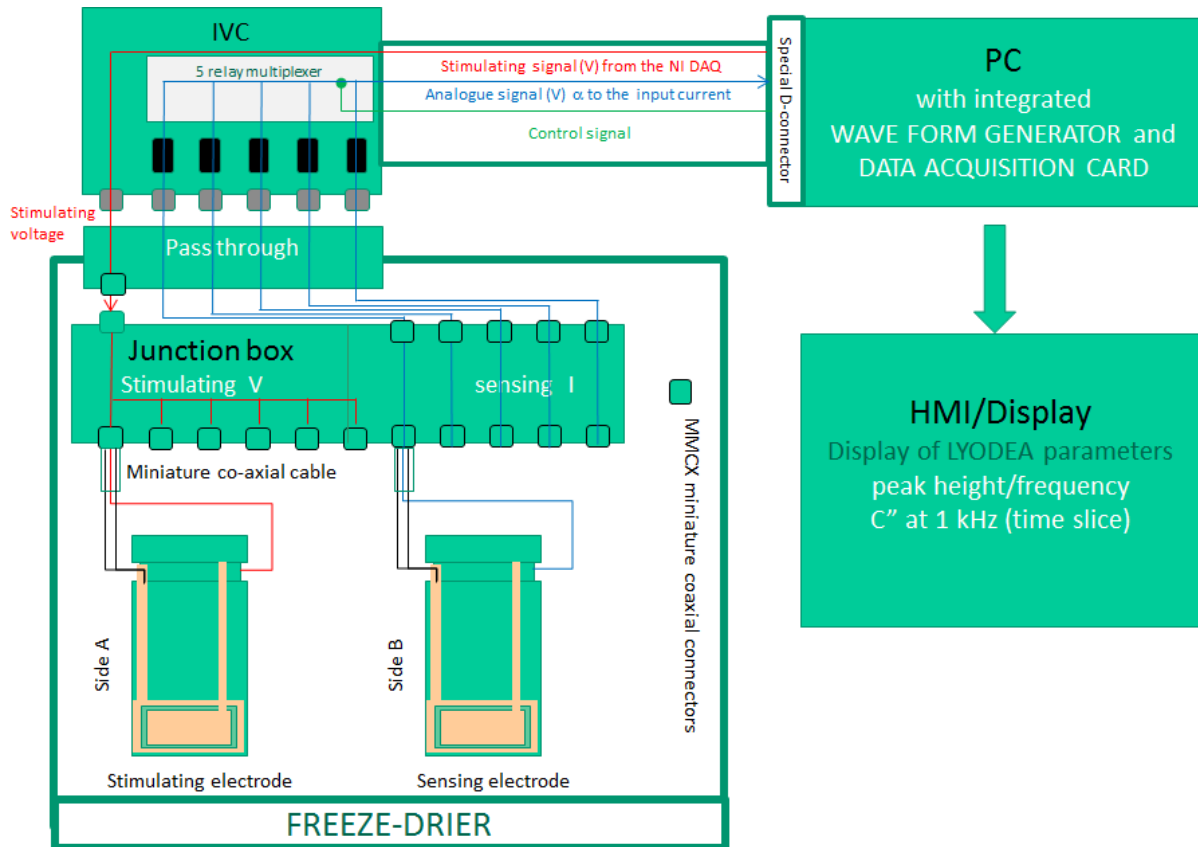
Figure 1 Block diagram of the impedance measurement system. Sides A and B are part of the same vial.

The technology combines the function of different single vial PATs (viz. thermocouple and microbalances) but with a number of advantages: the measurement electrodes are non-intrusive to the product volume or head space (un-like a thermocouple) which means that the system will not interfere with the processes of ice nucleation and growth. The measurement hardware has minimal thermal mass and volume (unlike the microbalance). This minimises the impact on heat transfer while facilitating measurements on vials which are arranged in the usual hexagonal array (a requirement for maximising the number of vials loaded into the freeze-dryer). Although the present design of impedance measurement vials does not support automatic loading, the use of thin foil electrode makes the tests vials suitable for their placement at any position within the hexagonal array. This feature, in turn, suggests the potential application of TVIS in spatial mapping of the shelf. A multichannel (TVIS) instrument design enables the placement of impedance measurement vials at

339   different positions across the shelf which can map the shelf for temperature distributions and

340   variations in the drying rates and to guard against the potential for product collapse.

341   **Electrical Impedance**

342   The electrical impedance of a material determines how easily the material will conduct a current

343   when an alternating voltage is applied to it. Electrical impedance is a function of both the dielectric

344   and conductive properties of the material which are in turn defined by the temperature,

345   composition and physical state of the material contained within the vial (an example TVIS vial is

346   shown in Figure 2i). Changes in these electrical parameters therefore directly mirror the condition of

347   the sample and the progression of the freeze-drying cycle. In order to explain the observed

348   impedance spectrum of the object under test and relate it to the physical properties or changes that

349   may happen during the freeze-drying process, it is necessary to create an appropriate equivalent

350   circuit model. The circuit model (Figure 2 ii) was found to provide an approximate fit to the

351   measured impedance spectrum, where C_G signifies the electrical capacitance of the glass walls of a

352   vial, which is charged through the resistance (R_S) representing the conductivity of the sample, and C_S

353   represents the electrical capacitance of the material within the internal volume of a vial. This imparts

354   a frequency-dependence to the measured dielectric properties, such that the capacitance of the

355   glass wall (C_G) will have sufficient time to charge completely at low frequency, but at high frequency,

356   will not have time to begin to accumulate any of the electrical charge that could otherwise be

357   accommodated.
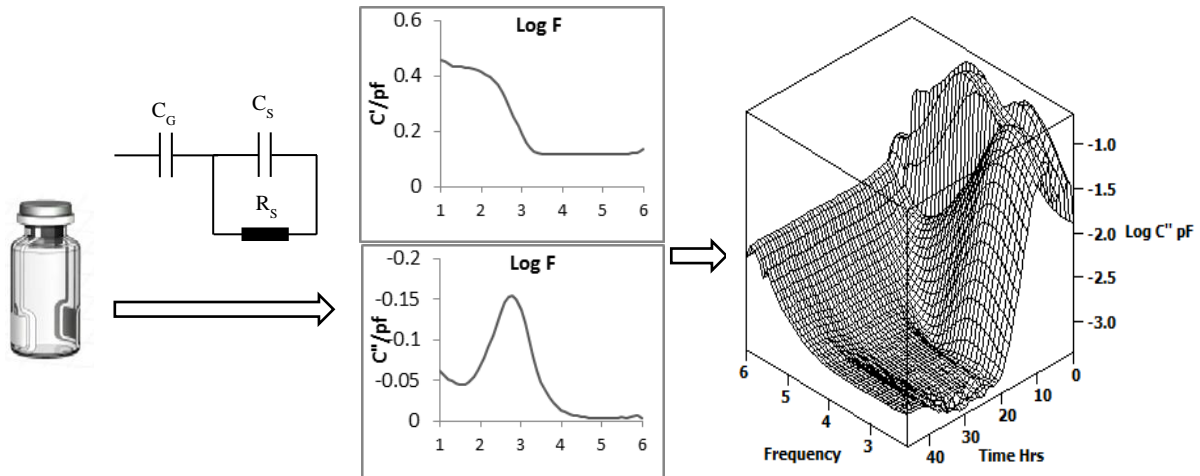
Figure 2 Description of measurement principles; from left to right (i) TVIS measurement vial with external electrodes attached (in this particular variant there are guard electrodes around each of the measurement electrodes), (ii) equivalent electrical circuit, with C_G modelling the capacitance of the glass wall of the vial, and C_S and R_S modelling the capacitance and resistance of the contents of the vial, (iii) individual spectrum (C' vs log frequency is the real part spectrum, C" vs log f is the imaginary part spectrum) where the frequency of the peak in the imaginary capacitance is given by $f = 1/2\pi R_S(C_G + C_S)$ (Note that this particular spectrum is taken after freezing the sample), and (iv) response surface plot of imaginary capacitance, resulting from measurements at a range of temperatures. The peak at position A in the early stages of the cycle shows the condition of the sample in the liquid state. The peak shifts to position B (lower frequencies) when the sample freezes and the product resistance increases by a factor of 100-1000. The decrease in the peak height over time is a consequence of the loss of ice on sublimation during the primary drying phase. The wing at low frequency (shaded area D delineated by the dotted line) is more than likely to be due to the additional distributed element characteristics of the glass wall.

The overall result is that the capacitance spectrum of the material under test (i.e. glass vial, its contents, and the electrical connections to the vial) will display a step-like decrease in capacitance as the frequency is increased through that critical frequency which corresponds to the time constant for the sample ($f = 1/2\pi\tau$, where $\tau = R_S(C_G + C_S)$) (Figure 2 iii top). There is a corresponding peak in the associated imaginary capacitance spectrum as the material under test starts to conduct electricity through the phase lag between the response of the sample and the applied electric field (Figure 2 iii bottom). The step in the real part capacitance and the peak in the imaginary capacitance are the manifestation of what is known as an interfacial-relaxation process. It is a consequence of the time dependence of the accumulation of charge at the glass surface as ions migrate through the liquid (or solid) contained within the glass vial, following the application of an external field [44].

It is the characteristics of this process that are used to 'follow' the progression of the freeze-drying cycle. More specifically, it is the peak frequency and peak value for the imaginary capacitance (which

384   can be considered as the magnitude of the interfacial-relaxation process) that is used to monitor the

385   freeze-drying cycle. Figure 2iv shows a typical surface plot of the imaginary capacitance as a function

386   of frequency and time, during the entire freeze-drying cycle. There are characteristic shifts in the

387   relaxation frequency and change in the peak height as the temperature of the sample changes and

388   when the material undergoes a phase change (e.g. liquid to ice) [45]. There is then a dramatic

389   decrease in the magnitude of the interfacial-relaxation peak as ice is removed from the sample.

390   Factors such as salt content, buffers and tissue culture medium will increase the conductivity and

391   shift the relaxation peak to the higher frequency end of the experimental frequency window.

392   The impedance of the object under test (namely the glass vial and its contents) can be calculated

393   from the following equation

394
$$Z^* = \frac{1}{i\omega C*} = \frac{1}{i\omega C_G} + \frac{1}{\frac{1}{R_S} + i\omega C_S} \tag{1}$$

395   From the complex impedance formula, the expressions for real and imaginary capacitance can be

396   calculated to explain the origin of interfacial polarization peak

397
$$Z^* = \frac{1}{i\omega C_G} + \frac{R}{1 + i\omega R_S C_S} = \frac{1 + i\omega R(C_S + C_G)}{i\omega C_G - \omega^2 R_S C_S C_G} \tag{2}$$

398
$$C^* = \frac{1}{i\omega Z^*} = \frac{C_G + i\omega R_S C_S C_G}{1 + i\omega R_S(C_S + C_G)} \tag{3}$$

399   By multiplying nominator and denominator by the complex conjugate of denominator

400
$$C^* = \frac{1}{i\omega Z^*} = \frac{(C_G + i\omega R_S C_S C_G)(1 - i\omega R_S(C_S + C_G))}{(1 + i\omega R_S(C_S + C_G))(1 - i\omega R_S(C_S + C_G))} \tag{4}$$

401
$$= \frac{C_2 + \omega^2 R_S^2 C_S C_G(C_S + C_G) - i\omega R_S C_G^2}{1 + (\omega R_S((C_S + C_G))^2} \tag{5}$$

402   and grouping the real and imaginary members decomposes C* into its real C' and imaginary parts

403
$$C' = \frac{C_G + \omega^2 R_S^2 C_S C_G(C_S + C_G)}{1 + (\omega R_S((C_S + C_G))^2} \tag{6}$$

404   and

405
$$C'' = -\frac{\omega R_S C_G^2}{1+(\omega R_S((C_S+C_G))^2}$$
(7)

406 For an example spectrum (Fig. 2) at $\omega \to 0$, $C'' = 0$.

407 As the frequency is increased, C'' increases to a maximum of

408
$$C''_{max} = \frac{C_G^2}{2(C_S+C_G)}$$
(8)

409 at a frequency of

410
$$\omega_{max} = \frac{1}{R(C_S+C_G)}.$$
(9)

411 and then decreases to 0 as the frequency $\omega \to \infty$

412 The value of the real part of capacitance at $\omega \to 0$ is $C' = C_G$

413 and the value at $\omega \to \infty$ is

414
$$C' = \frac{C_S C_G}{(C_S+C_G)}.$$
(10)

415 It follows that the step change in capacitance is

416
$$\Delta C' = C_G - \frac{C_S C_G}{(C_S+C_G)}, \text{ or } \Delta C' = \frac{C_G^2}{(C_S+C_G)}.$$
(11)

417

418 **Measurement of sublimation rate and end of primary drying**

419 The basic assumption is that the capacitance is a function of the amount of ice in the measurement

420 vial and provides the rationale for the application of TVIS as a determinant of ice sublimation rate

421 during primary drying. It has been demonstrated that TVIS can be used to measure the onset of

422 primary drying, rate of ice sublimation and end of primary drying [42].

423 Equation 12 (and the explanation that follows) demonstrates how the magnitude of the peak in the

424 imaginary part capacitance, during primary drying, provides an assessment of the remaining ice and

425   thereby an opportunity to assess relative drying rates in vials as the process is scaled-up from the

426   mini-piloting study (e.g. on an individual vial or a small cluster of vials).

427
$$C''_{max} = \frac{C_G^2}{2(C_S+C_G)}$$
(12)

428   The magnitude of each lumped circuit element $(C_S + C_G)$ is proportional to the cell constant for that

429   element, i.e.

430
$$C_G = \varepsilon_G \varepsilon_0 \frac{A}{d}$$
(13)

431   and

432
$$C_S = \varepsilon_S \varepsilon_0 \frac{A}{d}$$
(14)

433   where A is the area of interface between the frozen mass and the glass adjacent to the electrode.

434   Provided the sublimation interface is flat then as the ice is removed from the sample and the

435   sublimation front recedes down the vial, then the interfacial area between the frozen layer and the

436   juxtaposed glass wall (A) will decrease in proportion to the remaining ice volume. An electrical

437   model of the drying process is given in Figure 3, in which a dry-layer impedance is incorporated into

438   the overall impedance of the system. In reality, the impedance of this layer can be ignored given that

439   the time constant for charging the segment of glass in proximity to the dry layer is very large, owing

440   to the high resistance of the dried solid, and the only contribution made will be a small contribution

441   to the real part capacitance.

442

443
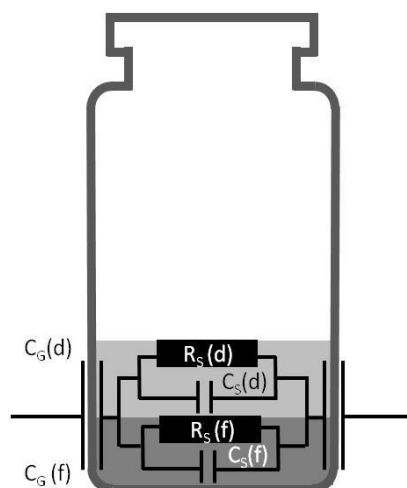
Figure 3 Equivalent circuit model of a two layer system, with a dry layer above an ice-rich layer. Here the
model shows an external electrode system that is of a height such that the fill volume extends both above the top
and below the base of the electrode.

447   The schematic in Figure 3 illustrates how the measured capacitance of the glass and the frozen

448   solution will change on drying. For a linear drying rate (in time) and for a flat sublimation interface,

449   both C_S and C_G would be expected to decrease in a linear response. However, given the fact that the

450   electrodes do not span the full height of the liquid one then needs to consider the impact of the

451   height of the frozen layer in relation to the electrode height on the measured response. It follows

452   that one can expect a greater sensitivity to the frozen layer in the middle/centre region of the

453   electrode than in the regions above and below the electrode. This feature of the measurement

454   system in its current form (with electrodes on the outside of the vial) partly explains why one

455   observes the sigmoidal decrease in the magnitude of the peak as the ice sublimes from the sample

456   (Figure 4).

457   To explore this observation further one needs to consider the fill volume/height in relation to the

458   vial size and electrode geometry being used (Although we might add that, in the classical scale up

459   approach in lyophilisation, one would keep the fill height the same but increase surface area in order

460   to increase drying rates). The theoretical impact of this change in vial geometry in relation to the

461   electrode geometry was explored in a previous publication, in which it was predicted that the

462   relaxation frequency might increase by up to a factor of two if 2 mL vials are used instead of the 10

463   mL vials we have used in our work [45].

464   In our case, the electrode height in the current presentation of the TVIS measurement system is 5

465   mm, which means that for a fill volume of 3 ml the liquid height is ~9.5 mm. The electrode is placed

466   in such a way that it is 1-2 mm above the vial base (measured externally) and is 2-3mm below the fill

467   height [45]. If there is a 1-2 mm gap (i.e. ice layer) below the electrode then there will be 2.5 to 3.5

468   mm of ice layer above the electrode. It follows that the response of the TVIS spectrum to a reduction

469   in the height of the ice layer won't be registered until (2.5-3.5)/9.5 (i.e. 25 to 35%) of the ice is

470   removed. The data generated by the TVIS system supports this observation (Figure 5) which shows

471   that the TVIS system only begins to register the loss of ice when the ice has reduced to

472   approximately 20%. Thereafter, the TVIS system senses a linear decrease in the magnitude of the

473   peak after approximately 40% of the ice has been removed.

474   Extrapolation of the linear portion of the C''_{peak} vs time plot, to the start of the primary drying phase,

475   suggests that a surrogate drying rate may be determined from the imaginary capacitance alone,

476   thereby facilitating comparison between vials placed in different position in the dryer.
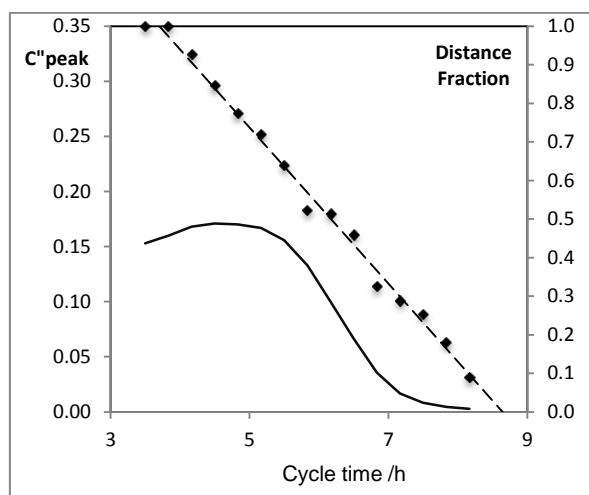
Figure 4 Capacitance profile of 3% w/v lactose during primary drying; the solid line is C''_{peak} vs primary drying as measured by the TVIS system. The symbols and the long dashed line is the loss of ice as determined from a visual assessment of the ice layer from the outside of the vial. The short dotted lines on the linear region of the C''_{peak} plot is the surrogate drying rate determined by the TVIS system.

It remains to be seen whether any general rules may be developed which enables the drying rate of a range of formulations to be extracted from TVIS measurements. For example, what is unknown at present is the amount of ice that has formed. This uncertainty may be removed by calculating the water content of the unfrozen layer from a measurement of the glass transition temperature (see following section) and the application of the Gordon-Taylor equation. A more straightforward application of this methodology would be to use it to evaluate the heat transfer coefficient (K_v) at the base of the vial from a sublimation experiment using water (rather than the product solution). Other parameters to be recorded, in order to achieve a clear evidence of the sublimation rate, include the measurement of temperature at the vial bottom and cake resistance to vapour flow. In that case the amount of ice is known as it is the same as the amount of water that is added to the vial [46].

Examples of the use of TVIS in mini-piloting (from single to multiple vials) to measure temperature and to characterise critical temperatures and transitions

In the sections that follow a number of applications for TVIS have been described in order to demonstrate the versatility of the technique in the characterization of first and second order phase

497   transitions (ice formation, eutectic formation and suppression, glass transitions and phase

498   separation), product temperature, and product collapse.

499   In the majority of the following applications, the sensitivity of the TVIS response surface to changes

500   in the resistance of the fill solution have been exploited to determine changes in state (e.g. liquid to

501   solid) and the temperature of the solution (whether liquid or frozen). From equation 9 (re-stated

502   here)

503
$$\omega_{max} = \frac{1}{R(C_S + C_G)} \tag{9}$$

504   one can see the impact of a phase change, which increases the resistance of the sample by a factor

505   of 100-1000 whereas the capacitance will only change by a factor of 25% at best (e.g. 80 to 100). The

506   peak frequency is therefore strongly dependent on the sample resistance.

507   **Measurement of Eutectic crystallization**

508   Classically, eutectic crystallization of an excipient in a formulation is detected using off-line DSC

509   studies, however, until recently there were no techniques capable of recording the manifestation of

510   this crystallization process in-line and therefore it is unclear whether there is a need to include an

511   annealing stage in the drying cycle. The impedance measurements recorded from a surrogate

512   formulation containing mannitol demonstrates a secondary peak in the derivative of the resistance

513   profile at ~-22 °C which was in close agreement with the eutectic crystallization of mannitol as

514   determined by DSC (Figure 5).
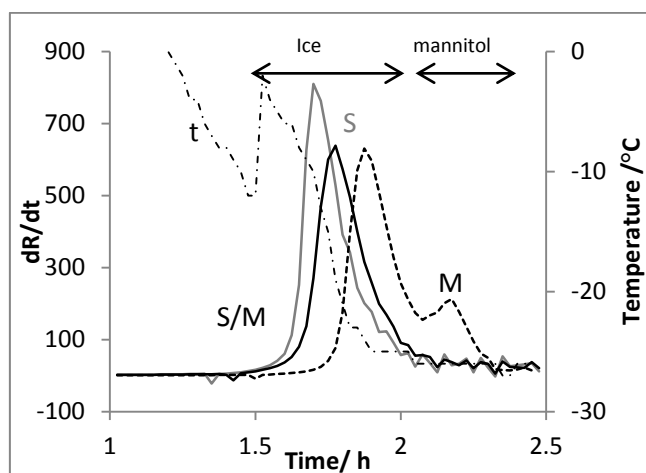
515

516 **Figure 5** The electrical resistance (dR/dt) profile during freezing of mannitol solution (M), sucrose (S) and a
517 50:50 mixture of mannitol and sucrose (S/M)

518 During this study, the impact of a non-crystallizing solid (sucrose) was also shown to suppress the

519 crystallizing behaviour of mannitol [47].

520 **Measurement of product collapse**

521 It is well known fact that the viscosity of a formulation decreases as the temperature increases

522 above glass transition T_g'. At some temperature exceeding T_g', the viscosity of the frozen formulation

523 is insufficient to hold its own weight and the product collapses; the corresponding temperature is

524 called collapse temperature (T_C) [48]. The measurement of structural collapse in a product during

525 primary drying remains a challenge for the formulation scientist. In essence, it may provide a realistic

526 value of temperature that defines the boundary of a design space.

527 Conventionally, T_C is measured by freeze drying microscopy which measures the drying front of small

528 sample positioned at the temperature controlled freeze drying stage under vacuum [24]. This

529 temperature is then considered as the upper temperature limit for the primary drying stage.

530 Recently, Mujat and co-workers used an optical coherence tomography based freeze drying

531 microscopy (OCT FDM) to record collapse temperature of a surrogate formulation [25, 49]. The

532 technology is advantageous as it records in-vial measurements of product collapse within a bespoke

533 design of a single vial freeze dryer. The results from this study indicate that T_c measured by OCT FDM

534 was ~3°C higher than the one measured by conventional FD microscopy suggesting a higher primary

535 drying temperature is permissible that could reduce the primary drying time by up to 30%. Although

536 the OCT FDM system measures the response of the frozen solution within the glass vial, there are

537 certain limitations such as: (i) only part of the formulation in direct contact with the probe is

538 measured, (ii) the presence of the probe may perturb the ice structure and (iii) it is not possible to

539 use the measurement system on vials placed within the usual configuration of a hexagonal array.

540 In a previous study [44], impedance spectroscopy has been used to record a sudden change in the

541 capacitance (Fig. 6) which is associated with the macroscopic structural collapse of product (as

542 measured by photographic images). This observation suggests a useful application of the TVIS in

543 recording a failure mode.
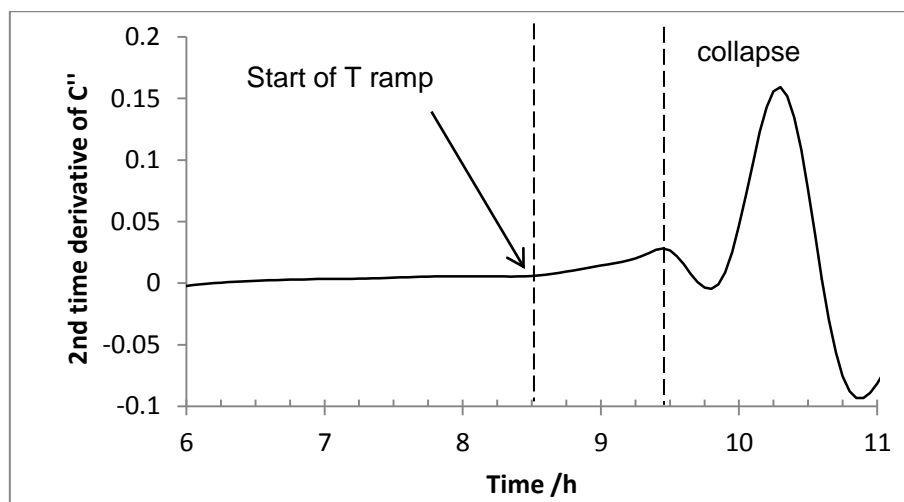
544

545 **Figure 6** Demonstration of collapse in 3% solution of sucrose as the shelf temperature is increased during the
546 primary drying phase.

547 **Measurement of the glass transition**

548 TVIS has been reported as a direct measurement approach which effectively measures in-vial glass

549 transition temperatures during re-heating post freezing (Figure 7)[47].
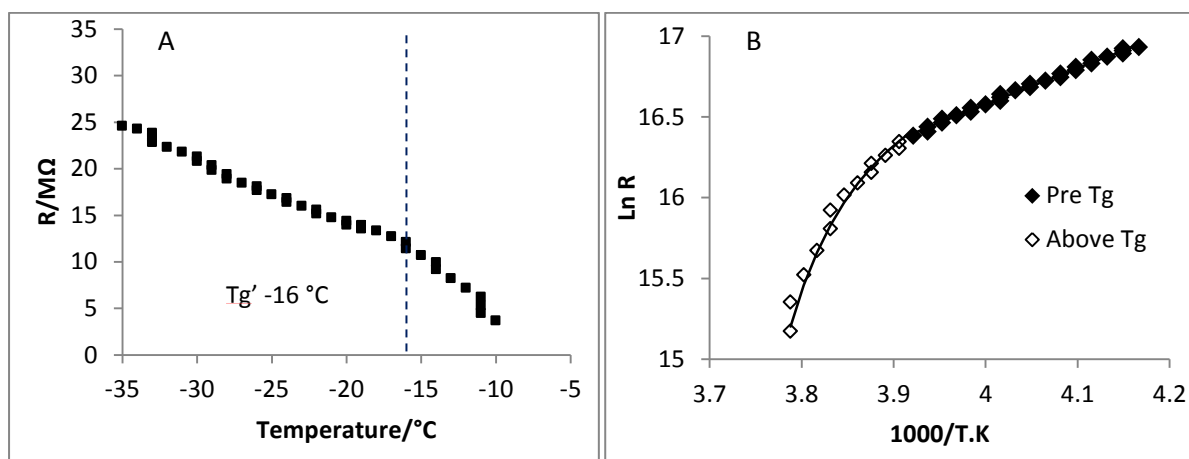
Figure 7 Electrical impedance profile of 10% w/v maltodextrin DE16-19 during re-heating. A) Temperature profile of equivalent circuit parameter R showing an inflection at the glass transition temperature of −16 C; B) Arrhenius plot of ln R vs 1000/T showing Arrhenius behaviour below T_G and non-Arrhenius behaviour above T_G (the solid line is the VTF model).

The additional benefit of this approach is that the impedance data can be modelled with a modified VTF (Vogel-Tammann-Fulcher) equation which can be employed to calculate the fragility of the frozen glass. This observation refers to an additional application of TVIS for formulation screening (especially for micro-plate/min-vial scale) and the potential for validation of formulation behaviour when transferred to into the process development stage (mini-piloting to scale-up). This parameter is likely to find application in determining the changes in the strength of the frozen glass following annealing which might impact the stability of the product. Such information may also provide additional information on the rationale for the inclusion of annealing step in the freeze drying cycle [50].

Temperature measurements

Figure 8 shows that there are correlations between log F_{peak} and product temperature during product cooling in the liquid state (A to B) and the solid state (C to D) and on annealing (D to E). The temperature coefficient for log F_{peak} in the frozen state (D to E) is ~0.04 which is approx. x3 of the temperature coefficient in the solution state.

569   By fitting the equivalent circuit in Figure 2ii to the calibration model data in the region D to E, it is

570   then possible to estimate the impact that a temperature gradient, within the vial (from the base to

571   the top of the ice layer) will have on the spectra acquired during primary drying.

572
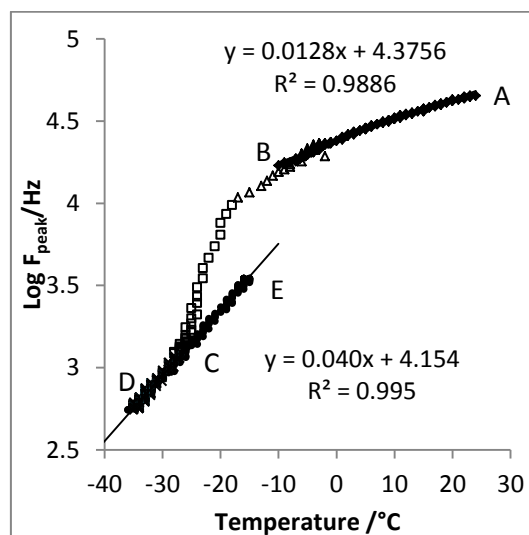
Figure 8 Temperature calibration of the TVIS instrument, the relationship between log F_{peak} and temperature is
linear, both in the liquid state (A to B) and the frozen state (C to D to E). Fitting the equivalent circulate model
to the data in the region C to D to E provides an opportunity to create a model for the scenario when there may
be differences in temperature between the top and bottom of the ice layer during primary drying.

577   To this end an equivalent circuit model was built comprising a number of horizontal segments

578   (Figure 10) with each segment comprising a parallel combination of a capacitor and a resistor.

579   Estimates for each element were taken from the calibration data represented in Figure 9, having

580   taken into account the fact that the cell constants for each segment were now a fraction of the cell

581   constant for the entire volume of the sample (in the case of the capacitive element) and a multiple

582   of the cell constant for the entire volume of the sample (in the case of the resistive element).

583
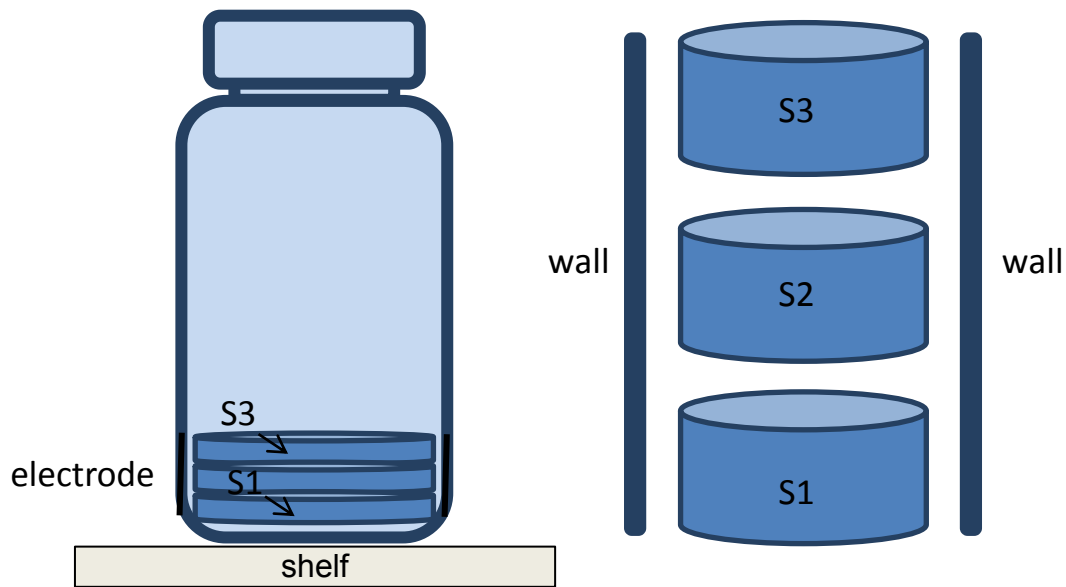
$$C_n{}^*(i\omega) = \frac{1}{R_n} + i\omega C_n \ (n = 1 \text{ to } 3)$$
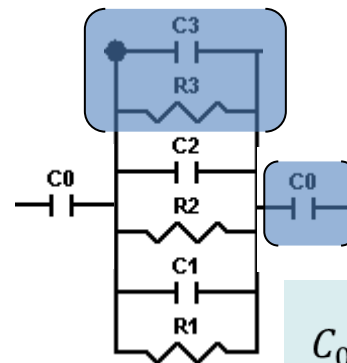
$$C_0{}^*(i\omega) = \frac{1}{i\omega C_0}$$

584

585

586 **Figure 9** Illustration of how to create a distributed circuit model to account for temperature differences between the top and bottom layers of the frozen solution. Here three
587 horizontal segments have been used to model a difference in temperature. In each segment the values for the lumped circuit elements have been taken from the calibration
588 model in the frozen state (Data from region C to E

589
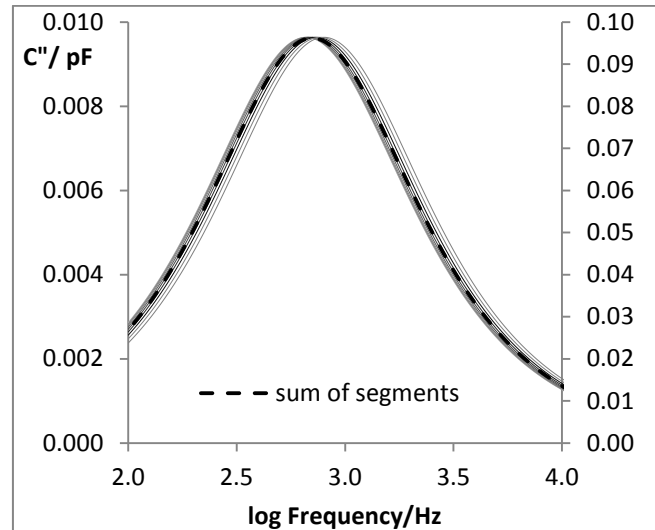
590

596 Results from the model (Figure 10) suggests that the shape of the spectrum does not change when

597 there is a distribution of temperatures across the frozen layer and that the peak frequency provides

598 an indication of the mean temperature of the frozen mass (dashed line on Figure 10). The mean

599 temperature may in itself be usefully employed as the driver to set the shelf temperature in a

600 process control scenario. In the development cycle, one might instead want to include a

601 thermocouple in the base of the vial to measure the base temperature and then use the TVIS

602 derived mean temperature to predict the temperature at the sublimation interface. That would

603 require the assumption that the profile across the frozen layer was linear.

Characterization of Annealing

605 The inclusion of annealing step increases mass transfer rates during primary drying [51] as it

606 overcomes ice crystal heterogeneities which arise from uncontrolled freezing a stochastic process,

607 by promoting the growth of large ice crystals which in turn reduces the dry later resistance. An

608 annealing step is also included to promote crystallization of bulking agent such as mannitol. TVIS has

609　been used to improve our understanding of how drying rate changes with the annealing hold time

610　and temperature (Fig. 11) [52].
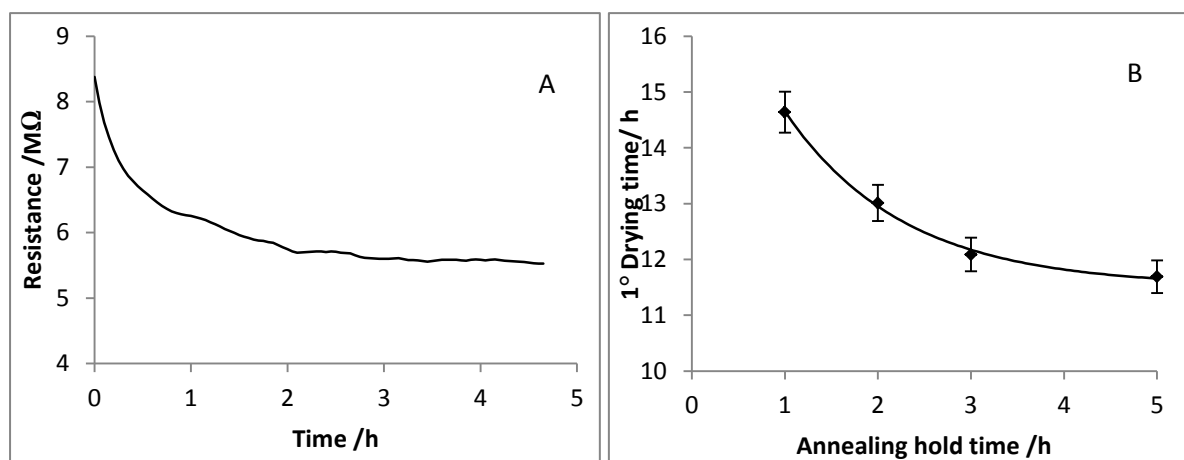
611

612　**Figure 11** A) Resistance profile of maltodextrin 10% w/v during annealing hold time B) Impact of annealing
613　hold time on the drying time

614　By recording the changes in electrical impedance of the formulation during annealing as well as the

615　primary drying stage of the freeze drying cycle, it was possible to demonstrate that Ostwald ripening

616　was the primary mechanism responsible for faster drying rate. Devitrification, the other mechanism

617　in question, was ruled out as there was no significant amount of additional ice formation recorded

618　as glass transition temperature was not increased following annealing.

619　The crystal growth occurs at exponential rates and this phenomenon is almost complete after 3h.

620　Any extension to this hold time in excess of 3 h is largely unjustified as the sublimation rate does not

621　increase accordingly and these observations are in agreement with the R profile during annealing

622　which records asymptote after an annealing hold time of 3h.

623　**Phase separation**

624　In certain cases, the formulation components exhibit physical incompatibility in that different phases

625　separate out from the solution during freezing and are subsequently dried as separate layers. In

626　order to demonstrate the potential use for through vial impedance measurement in the

627　determination of phase separation, a binary solution of 14% w/w dextran (MW 9-11000) (Sigma) and

628 14% w/w polyvinylpyrrolidone PVP K10 (Sigma) was analysed over a frequency range 100Hz-1MHz at

629 scan interval of 0.5 min^{-1} throughout the following freezing cycle: Temperature ramp to -35 °C in 60

630 minutes, hold then at -35 °C for 120 minutes and temperature ramp up from -35 °C to 25 °C in 60

631 minutes using a HETO FD 08 freeze dryer. The product temperature was also recorded in a

632 neighbouring vial using a type K thermocouple. Thermal analysis of the formulation was also

633 performed by differential scanning calorimetry, scanning over the same temperature range.

634 After fitting the impedance model in equation 1 to each spectrum, the time derivative of values of

635 the element R_S was seen to undergo a non-linearity with temperature, which was a direct

636 consequence of the sample passing through a glass transition. Time derivatives of the R_S parameter

637 provided estimates for T_g' of -13 °C and -24 °C, whereas the T_g' estimates from DSC are -13 °C and -

638 19.5 °C (Figure 12) the latter was in agreement with T_g' of individual components reported the

639 literature [53, 54].

640

641

642
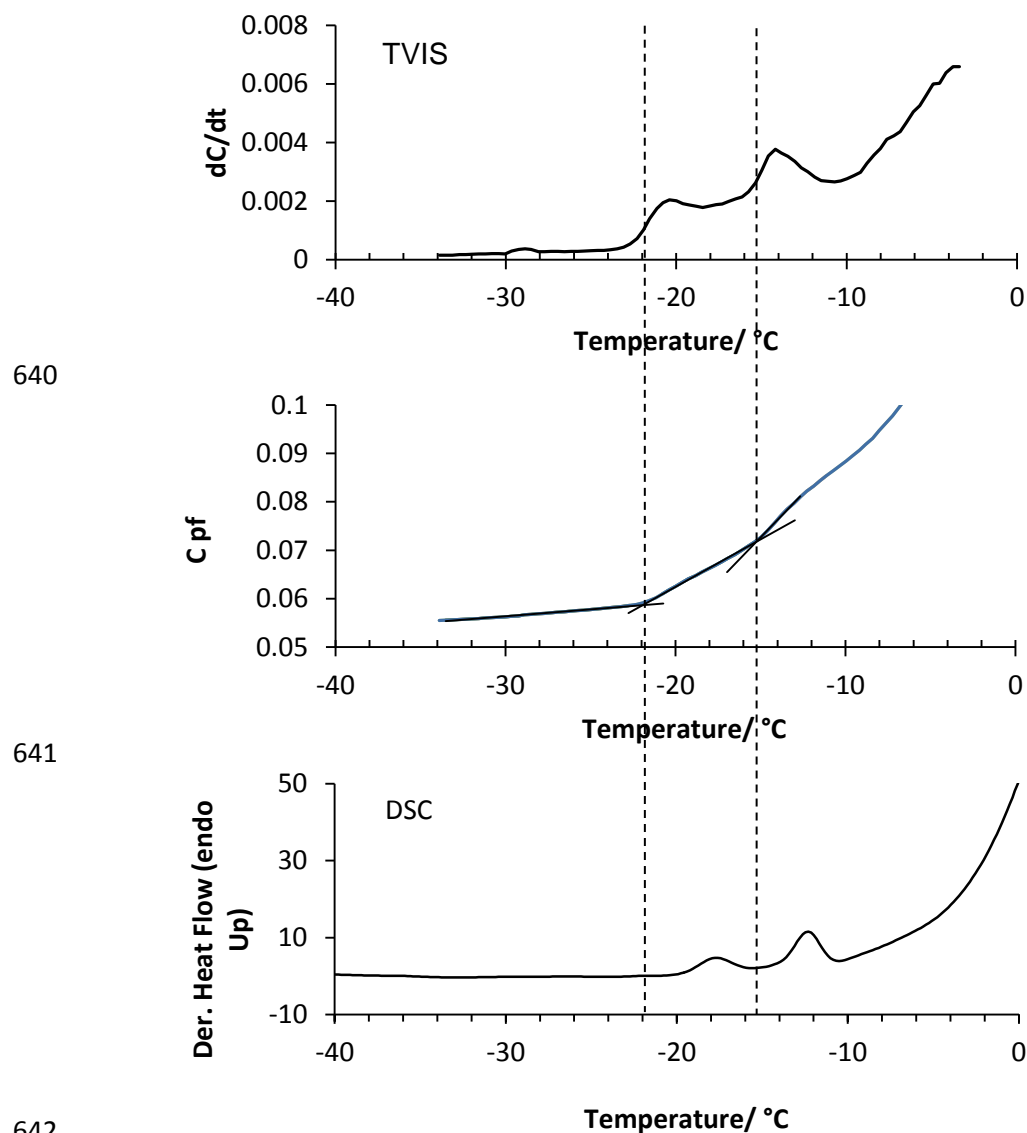
Figure 12 Time derivative and imaginary capacitance of 14% w/w dextran and 14% w/w PVP (b) DSC scan
during re-heating from -35 to 25 °C

645   The close agreement between the two values for the T_g' of the dextran phase (at -13 °C) points to

646   the reliability of the new method, whereas the disagreement between the two estimates for the

647   second T_g' may point to real differences in the composition of the PVP phase.

648   **Conclusions**

649   We have reviewed the advantage and limitation of the various available PAT technologies, such as

650   thermocouples, TDLAS and MTM, commonly used to monitor the freeze drying process. The

651   translation of process understanding from the mini-pilot to scale up and production demands a new

652 PAT method that can bridge these scales and provide the verification that the process parameters at

653 one scale can be achieved at another. TVIS provides part of that solution on the basis of a two

654 parameter measurement: The first parameter is the measurement of the magnitude of the

655 interfacial relaxation process which has been shown to provide a convenient non-invasive (albeit

656 single vial) measurement of drying rates. The second is the frequency position of the interfacial

657 relaxation which is sensitive to both temperature and phase behaviour. The most important critical

658 product parameter is the product temperature at the ice sublimation interface, T_p, as it defines the

659 efficiency of the process in terms of the rate of drying. Here we demonstrate a possible

660 methodology for determining simultaneously the critical process parameter and the impact it has on

661 drying rates. In future, with TVIS capability embedded in different scales or dryer, it should be

662 possible to track the product temperature and drying rate vs. time profile so that the influence of

663 process- and equipment-related differences may be first understood and then compensated for, and

664 a dynamic cycle developed which adapts the shelf inlet temperature and chamber pressure to

665 maintain this profile. Other capabilities of the TVIS method in the determination of the glass

666 transition and the strength/fragility of the unfrozen phase have been highlighted and suggestions

667 provided as to the relevance these parameters have in assessment of product stability.

668 **References**

669 1. Tang X, Pikal M. Design of Freeze-Drying Processes for Pharmaceuticals: Practical Advice. Pharm
670 Res. 2004;21(2):191-200. doi:10.1023/b:pham.0000016234.73023.75.
671 2. Brulls. M, Rasmuson. A. Heat transfer in vial lyophilization. Int J Pharm. 2002;246:1-16.
672 3. Guttzeit M. Designing An Effective PAT-Driven Scale-Up Of Lyophilization Processes
673 PharmTechnol. 2010;22(11):8.
674 4. Grant. Y, Dalby. PA, Matejtschuk. P. Use of Design of Experiment and Microscale Down Strategies
675 in Formulation and Cycle Development for Lyophilization. Am Pharm Rev. 2012:11.
676 5. Schwegman JJ, Hardwick LM, Akers MJ. Practical Formulation and Process Development of Freeze-
677 Dried Products. Pharm Dev Technol. 2005;10(2):151-73. doi:doi:10.1081/PDT-56308.
678 6. Kim AI, Akers MJ, Nail SL. The physical state of mannitol after freeze-drying: effects of mannitol
679 concentration, freezing rate, and a noncrystallizing cosolute. J Pharm Sci. 1998;87(8):931-5.
680 doi:10.1021/js980001d.
681 7. Kochs M, Körber C, Heschel I, Nunner B. The influence of the freezing process on vapour transport
682 during sublimation in vacuum-freeze-drying of macroscopic samples. Int J Heat Mass Transfer.
683 1993;36(7):1727-38. doi:http://dx.doi.org/10.1016/S0017-9310(05)80159-0.

8. Rambhatla S, Tchessalov S, Pikal M. Heat and mass transfer scale-up issues during freeze-drying, III: Control and characterization of dryer differences via operational qualification tests. AAPS PharmSciTech. 2006;7(2):E61-E70. doi:10.1208/pt070239.

9. Konstantinidis AK, Kuu W, Otten L, Nail SL, Sever RR. Controlled nucleation in freeze-drying: Effects on pore size in the dried product layer, mass transfer resistance, and primary drying rate. J Pharm Sci. 2011;100(8):3453-70. doi:10.1002/jps.22561.

10. Rasetto V, Marchisio DL, Fissore D, Barresi AA. On the use of a dual-scale model to improve understanding of a pharmaceutical freeze-drying process. J Pharm Sci. 2010;99(10):4337-50.

11. Ganguly A, Nail SL, Alexeenko A. Experimental determination of the key heat transfer mechanisms in pharmaceutical freeze-drying. J Pharm Sci. 2013;102(5):1610-25. doi:10.1002/jps.23514.

12. Patel SM, Pikal M. Process Analytical Technologies (PAT) in freeze-drying of parenteral products. Pharm Dev Technol. 2009;14(6):567-87. doi:doi:10.3109/10837450903295116.

13. Barresi AA, Pisano R, Fissore D, Rasetto V, Velardi SA, Vallan A et al. Monitoring of the primary drying of a lyophilization process in vials. Chem Eng Process. 2009;48(1):408-23.

14. Fissore D, Pisano R, Barresi AA. On the Methods Based on the Pressure Rise Test for Monitoring a Freeze-Drying Process. Drying Technol. 2010;29(1):73-90. doi:10.1080/07373937.2010.482715.

15. Bosca S, Barresi AA, Fissore D. Use of a soft sensor for the fast estimation of dried cake resistance during a freeze-drying cycle. Int J Pharm. 2013;451(1–2):23-33. doi:http://dx.doi.org/10.1016/j.ijpharm.2013.04.046.

16. Bosca S, Barresi BA, Fissore D. Use of soft sensors to monitor a pharmaceuticals freeze-drying process in vials. Pharm Dev Technol. 2012;0(0):1-12. doi:doi:10.3109/10837450.2012.757786.

17. Jameel F, Kessler WJ, Schneid S. Application of PAT in Real-time Monitoring and Controlling of Lyophilization Process. Quality by Design for Biopharmaceutical Drug Product Development. Springer; 2015. p. 605-47.

18. Grant Y, Matejtschuk P, Bird C, Wadhwa M, Dalby PA. Freeze drying formulation using microscale and design of experiment approaches: a case study using granulocyte colony-stimulating factor. Biotechnology letters. 2012;34(4):641-8. doi:10.1007/s10529-011-0822-2.

19. Kauppinen A, Toiviainen M, Korhonen O, Aaltonen J, Jarvinen K, Paaso J et al. In-line multipoint near-infrared spectroscopy for moisture content quantification during freeze-drying. Anal Chem. 2013;85(4):2377-84. doi:10.1021/ac303403p.

20. Capelle MAH, Gurny R, Arvinte T. High throughput screening of protein formulation stability: Practical considerations. Eur J Pharm Biopharm. 2007;65(2):131-48. doi:http://dx.doi.org/10.1016/j.ejpb.2006.09.009.

21. Kauppinen A, Toiviainen M, Aaltonen J, Korhonen O, Järvinen K, Juuti M et al. Microscale Freeze-Drying with Raman Spectroscopy as a Tool for Process Development. Anal Chem. 2013;85(4):2109-16. doi:10.1021/ac3027349.

22. Capelle MAH, Arvinte T. High-throughput formulation screening of therapeutic proteins. Drug Discovery Today: Technologies. 2008;5(2–3):e71-e9. doi:http://dx.doi.org/10.1016/j.ddtec.2009.03.003.

23. PSI. Lyoflux: Tunable Diode Laser Absorption Spectroscopy. Physical Sciences Inc., USA. 2016. http://www.psicorp.com/case-studies/lyoflux%E2%84%A2-tunable-diode-laser-absorption-spectroscopy. Accessed 20/06/2016 2016.

24. Meister E, Gieseler H. Freeze-dry microscopy of protein/sugar mixtures: Drying behavior, interpretation of collapse temperatures and a comparison to corresponding glass transition Data. J Pharm Sci. 2009;98(9):3072-87. doi:10.1002/jps.21586.

25. Mujat M, Greco K, Galbally-Kinney KL, Hammer DX, Ferguson RD, Iftimia N et al. Optical coherence tomography-based freeze-drying microscopy. Biomed Opt Express. 2012;3(1):55-63.

26. De Beer T, Burggraeve A, Fonteyne M, Saerens L, Remon JP, Vervaet C. Near infrared and Raman spectroscopy for the in-process monitoring of pharmaceutical production processes. Int J Pharm. 2010;In Press, Corrected Proof.

735 27. De Beer TRM, Vercruysse P, Burggraeve A, Quinten T, Ouyang J, Zhang X et al. In-line and real-
736 time process monitoring of a freeze drying process using Raman and NIR spectroscopy as
737 complementary process analytical technology (PAT) tools. J Pharm Sci. 2009;98(9):3430-46.
738 doi:10.1002/jps.21633.
739 28. Pikal MJ, Shah S, Roy ML, Putman R. The secondary drying stage of freeze drying: drying kinetics
740 as a function of temperature and chamber pressure. Int J Pharm. 1990;60(3):203-7.
741 29. Hsu CL, Heldman DR, Taylor TA, Kramer HL. Influence of Cooling Rate on Glass Transition
742 Temperature of Sucrose Solutions and Rice Starch Gel. J Food Sci. 2003;68(6):1970-5.
743 doi:10.1111/j.1365-2621.2003.tb07003.x.
744 30. Pomerantsev AL, Rodionova OY. Process analytical technology: a critical view of the
745 chemometricians. Journal of Chemometrics. 2012;26(6):299-310. doi:10.1002/cem.2445.
746 31. Tang X, Nail S, Pikal M. Evaluation of manometric temperature measurement (MTM), a process
747 analytical technology tool in freeze drying, part III: Heat and mass transfer measurement. AAPS
748 PharmSciTech. 2006;7(4):E105-E11. doi:10.1208/pt070497.
749 32. Gieseler H, Kramer T, Pikal M. Use of Manometric Temperature Measurement (MTM) and
750 SMART^{TM} Freeze Dryer Technology for Development of an Optimized Freeze-Drying Cycle. J Pharm
751 Sci. 2007;96(12):3402-18.
752 33. Tang X, Nail S, Pikal M. Evaluation of manometric temperature measurement, a process
753 analytical technology tool for freeze-drying: Part II measurement of dry-layer resistance. AAPS
754 PharmSciTech. 2006;7(4):E77-E84. doi:10.1208/pt070493.
755 34. Johnson RE, Oldroyd ME, Ahmed SS, Gieseler H, Lewis LM. Use of manometric temperature
756 measurements (MTM) to characterize the freeze-drying behavior of amorphous protein
757 formulations. J Pharm Sci. 2009;99(6):2863-73. doi:10.1002/jps.22031.
758 35. Gieseler H, Kessler WJ, Finson M, Davis SJ, Mulhall PA, Bons V et al. Evaluation of tunable diode
759 laser absorption spectroscopy for in-process water vapor mass flux measurements during freeze
760 drying. J Pharm Sci. 2007;96(7):1776-93. doi:10.1002/jps.20827.
761 36. Kuu WY, Nail SL, Sacha G. Rapid determination of vial heat transfer parameters using tunable
762 diode laser absorption spectroscopy (TDLAS) in response to step-changes in pressure set-point
763 during freeze-drying. J Pharm Sci. 2009;98(3):1136-54.
764 37. Tang X, Nail SL, Pikal MJ. Freeze-Drying Process Design by Manometric Temperature
765 Measurement: Design of a Smart Freeze-Dryer. Pharm Res. 2005;22(4):685-700.
766 doi:10.1007/s11095-005-2501-2.
767 38. Schneid S, Gieseler H. Evaluation of a New Wireless Temperature Remote Interrogation System
768 (TEMPRIS) to Measure Product Temperature During Freeze Drying. AAPS PharmSciTech.
769 2008;9(3):729-39. doi:10.1208/s12249-008-9099-8.
770 39. Christ M. Lyocontrol-Sensor for process monitoring and for the determination of the freezing
771 point. In: Process control and optimization. Martin Christ, Germany. 2013. Accessed October 29
772 2013.
773 40. Luis Rey, May JC. Freeze-Drying/Lyophilization of Pharmaceutical and Biological Products. Drugs
774 and Pharamcaceutical sciences, vol 96. New York: Marcel Dekker; 1999.
775 41. Ward KR, Matejtschuk P. The Use of Microscopy, Thermal Analysis, and Impedance
776 Measurements to Establish Critical Formulation Parameters for Freeze-Drying Cycle Development.
777 In: Rey L, May JC, editors. Freeze Drying/Lyophilization of Pharmaceutical and Biological Products.
778 New york: Marcel Dekker; 2010. p. 112-35.
779 42. Smith G, Polygalov E, Arshad MS, Page T, Taylor J, Ermolina I. An impedance-based process
780 analytical technology for monitoring the lyophilisation process. Int J Pharm. 2013;449(1–2):72-83.
781 doi:http://dx.doi.org/10.1016/j.ijpharm.2013.03.060.
782 43. Smith G, Polygalov E, Page T, inventors; GEA Pharma Systems Limited, assignee. Electrical
783 monitoring of a lyophilization process Great Britain patent GB2480299. 2011 16/11/2011.

784 44. Smith G, Arshad MS, Polygalov E, Ermolina I, Nazari K, Taylor J et al. Through-Vial Impedance
785 Spectroscopy: A new in-line process analytical technology for freeze-drying. PharmTechnol.
786 2014;38(4):38-46.
787 45. Smith G, Arshad M, Polygalov E, Ermolina I. Factors Affecting the Use of Impedance Spectroscopy
788 in the Characterisation of the Freezing Stage of the Lyophilisation Process: the Impact of Liquid Fill
789 Height in Relation to Electrode Geometry. AAPS PharmSciTech. 2014;15(2):261-69.
790 doi:10.1208/s12249-013-0054-y.
791 46. Pikal MJ, Roy ML, Shah S. Mass and heat transfer in vial freeze-drying of pharmaceuticals: Role of
792 the vial. J Pharm Sci. 1984;73(9):1224-37. doi:10.1002/jps.2600730910.
793 47. Arshad MS, Smith G, Polygalov E, Ermolina I. Through-vial impedance spectroscopy of critical
794 events during the freezing stage of the lyophilization cycle: The example of the impact of sucrose on
795 the crystallization of mannitol. Eur J Pharm Biopharm. 2014;87(3):598-05.
796 doi:http://dx.doi.org/10.1016/j.ejpb.2014.05.005.
797 48. Sun WQ. Temperature and viscosity for structural collapse and crystallization of amorphous
798 carbohydrate solutions. Cryo Letters. 1997;18:99-106.
799 49. Greco K, Mujat M, Galbally-kinney KL, Hammer DX, Ferguson RD, Iftimia N et al. Accurate
800 prediction of collapse temperature using optical coherence tomography-based freeze-drying
801 microscopy. J Pharm Sci. 2013;102(6):1773-85. doi:10.1002/jps.23516.
802 50. Smith G, Arshad MS, Polygalov E, Ermolina I. An application for impedance spectroscopy in the
803 characterisation of the glass transition during the lyophilization cycle: the example of a 10% w/v
804 maltodextrin solution. Eur J Pharm Biopharm. 2013;85(3 Pt B):1130-40.
805 doi:10.1016/j.ejpb.2013.08.004.
806 51. James A. Searles JFC, Theodore W. Randolph. Annealing to Optimize the Primary Drying Rate,
807 Reduce Freezing-Induced Drying Rate Heterogeneity, and Determine Tg in Pharmaceutical
808 Lyophilization. J Pharm Sci. 2000;90(7):872-87.
809 52. Smith G, Arshad MS, Polygalov E, Ermolina I. Through-Vial Impedance Spectroscopy of the
810 Mechanisms of Annealing in the Freeze-Drying of Maltodextrin: The Impact of Annealing Hold Time
811 and Temperature on the Primary Drying Rate. J Pharm Sci. 2014;103(6):1799-810.
812 doi:10.1002/jps.23982.
813 53. Wei W. Lyophilization and development of solid protein pharmaceuticals. Int J Pharm.
814 2000;203(1–2):1-60. doi:10.1016/s0378-5173(00)00423-3.
815 54. Izutsu K-i, Aoyagi N, Kojima S. Effect of polymer size and cosolutes on phase separation of
816 poly(vinylpyrrolidone) (PVP) and dextran in frozen solutions. J Pharm Sci. 2005;94(4):709-17.
817 doi:10.1002/jps.20292.

818

819